Spectrochimica Acta Part A 71 (2009) 1845–1850

Contents lists available at ScienceDirect

Spectrochimica Acta Part A: Molecular and Biomolecular Spectroscopy

journal homepage: www.elsevier.com/locate/saa

Spectral studies of Fe(III) complexes of dipodal tridentate chelating agents

Zafar Ahmad Siddiqi*, Sarvendra Kumar, M. Khalid, M. Shahid

Department of Chemistry, Aligarh Muslim University, Aligarh 202002, India

ARTICLE INFO

Article history:
Received 7 February 2008
Received in revised form 2 July 2008
Accepted 3 July 2008

Keywords:
Fe(III) complexes
Mössbauer spectra
Dipodal tridentate ligand
Magnetic moment
Electronic ligand field spectra

ABSTRACT

The dipodal ligands (Im) and (BIm) as well as complexes [FeLCl$_3$] [L = Im (**1**) and BIm (**2**)] have been prepared and studied using spectroscopic techniques. The magnetic moment, IR, electronic (ligand field), FAB-mass and NMR spectral data indicate a hexa-coordinate geometry around high-spin state Fe^{3+} where the ligands coordinate as a tridentate [N,N,N] chelating agent. ^{57}Fe-Mössbauer spectral data confirmed the presence of a ligand asymmetry around Fe^{3+} in a high-spin state electronic configuration ($t_{2g}{}^3$,$e_g{}^2$, $S = 5/2$) with nuclear transition Fe($\pm 3/2 \rightarrow \pm 1/2$) exhibiting Kramer's double degeneracy. The molecular computations provided the optimum energy perspective plots for the molecular geometries giving the important structural data.

1. Introduction

The investigations of the bonding characteristic of imidazole and imidazole-based ligands towards metal ions, owing to their extremely broad biological significances have been one of the main topics of bio-coordination chemistry. During the past three decades [1], many efforts have been made to characterise metal ion linkages at the active centers of metallo-proteins. The presence of this particular moiety as the active sites in various metallo-proteins or metallo-enzymes is related to a great variety of metabolic processes [1]. The use of low-molecular weight model compounds of these biological macro-molecules has proved to be very useful and in some cases the only possible way to visualize the binding modes, structures and functions of the active sites. A variety of imidazole containing ligands and their metal complexes, which can mimic structural features of metallo-proteins or metallo-enzymes, have been investigated [2–8]. The presence of additional substituents containing nitrogen and/or oxygen donors, beside the imidazole rings, has been reported [1] to alter strongly the structure and properties of their complexes. Tripodal ligands are especially suitable to assess the electronic and geometrical factors regulating the Cu-proteins [9,10]. Consequently, considerable investigations have been devoted [2–8] to study the structure and bonding features of bivalent metal complexes of polydentate imidazole-based tripodal ligands. Complexes of tetradentate tripodal ligands generally results in a coordinatively unsaturated penta-coordinate geometry having an additional water molecule or counter ion in the coordination sphere. The formation of actual five coordinate structures either square pyramidal or trigonal bipyramidal strongly depends on the ligands, viz. nature of the donor groups as well as the counter anions, symmetry of the ligand and the constitution of the pendent arms or substituents. Except for some pyridyl/thioether and pyridyl/amine containing compounds [11] most of the investigated tripodal ligands are structurally symmetrical i.e. having donor group at the same bond distances form the central atom. Earlier reports [11–14] indicate that the un-symmetric tripodal ligands having embedded rings of different sizes can be of great use. Such chelating agents tend to result in complexes, which can mimic [2] the structure for the active center of many natural occurring metallo-proteins.

In this article, we report the synthesis and characterisations on the less symmetric dipodal ligands [(Im) & (BIm)] and their complexes with Fe^{3+} ion.

2. Experimental

2.1. Materials

All the reagents used were of analytical grade. The solvents were purified by standard procedures before use [15].

2.2. Preparation of the ligands

2.2.1. Synthesis of bis(4,5-dihydro-1H-imidazol-2-yl-methyl) amine (Im)

Powdered iminodiacetic acid (8.0 g, 60.0 mmol) was mixed thoroughly with 1,2-diaminoethane (8.0 mL, 120.0 mmol) along with a few drops of *o*-phosphoric acid in a hard pyrex tube, then

---

* Corresponding author.
E-mail address: zafarasiddiqi@yahoo.co.in (Z.A. Siddiqi).

1386-1425/$ – see front matter. Crown Copyright © 2008 Published by Elsevier B.V. All rights reserved.
doi:10.1016/j.saa.2008.07.016

heated under N_2 atmosphere to a melt at 180 °C for about 2 h on an oil bath. The reaction mixture was slowly brought to room temperature, which gave a dark coloured wax like product. The wax was extracted with 100 mL methanol, filtered off and the dark coloured insoluble residue was discarded after washing with methanol. The methanol extract was dried under vacuum giving a yellow colour wax type product. It was kept for about 6 weeks in a desiccator over $CaCl_2$, which changed to a hard mass. The hard mass was crushed to a fine powder and was recrystallized from methanol [yellow colour, m.p. 142 °C, yield 8.6 g, 79%]. Anal. calc. for $C_8H_{15}N_5$: C, 53.03; H, 8.28; N, 38.67, found for (Im) C, 53.07; H, 8.34; N, 38.65, FAB-mass (*m*-nitrobenzylalcoho NBA, matrix): $[\mathrm{Im{-}2H + Bz_3}]^+$ ($m/z = 333$) $[\mathrm{Im + 2H + Bz_4}]^+$ ($m/z = 472$) $[\mathrm{Im + 2H + Bz_5}]^+$ ($m/z = 490$) $[\mathrm{Im{-}CH_2CH_2 + Bz_3}]$ ($m/z = 307$) $[\mathrm{Im{-}CH_2CH_2 + 2H + Bz_4}]^+$ ($m/z = 444$) $[\mathrm{Im{-}NH.CH_2CH_2.H + Bz_1}]^+$ ($m/z = 273$) $[\mathrm{Im{-}C.NH.N{-}CH_2CH_2 + Bz_4}]$ ($m/z = 413$) $[\mathrm{Im{-}C_2H_4(NH)N.C.CH_2.NH}]$ ($m/z = 218$); [Fragments for NBA matrix, appear at $m/z = 136$ (Bz_1), 137 (Bz_2), 154 (Bz_3), 289 (Bz_4) and 307 (Bz_5)]. ^1H NMR (CD_3OD, ppm) δ: 3.32 (t, 4H, $J_{H-H} = 5.6$ cps, $-CH_2-)_{im}$, 3.41 (t, 4H, $J_{H-H} = 5.8$ cps, $-CH_2-)_{im}$, 4.50 (*s*, 4H, $-CH_2-$). ^{13}C NMR (CD_3OD, ppm) δ: 161.4 $(C{=}N)_{im,}$ 53.3 ($-CH_2-N$), 34.5, 52.4 $(-CH_2-)_{im}$.

2.2.2. *Synthesis of bis(1H-benzimidazol-2yl-methyl)amine (BIm)*

It was prepared in an analogous manner as following: iminodiacetic acid (8.0 g, 60.0 mmol) and 1,2-diaminobenzene (13.0 g, 120.0 mmol) were ground and thoroughly mixed in a mortar as a fine homogeneous mixture. This mixture was taken in a pyrex tube along with a few drops of *o*-phosphoric acid. It was sealed under N_2 atmosphere then heated at 190 °C for 2 h immersed in an oil bath. On cooling brought to room temperature a dark coloured hard solid mass was obtained, which was crushed to fine powder. It was extracted in a magnetically agitated 500 mL of methanol, filtered off and the black residue was discarded. The brown colour extract was evaporated to dryness under vacuum to give microcrystalline solid. The solid was recrystallized from methanol [pink colour, m.p. 160 °C, yield 10.80 g, ~65%]. Anal. calc. for $C_{16}H_{15}N_5$: C, 69.31; H, 5.41; N, 25.27. Found for (BIm): C, 69.34; H, 5.29; N, 25.29. FAB-mass of BIm (*m*-nitrobenzylalcoho NBA, matrix): $[\mathrm{BIm + H}]^+$ ($m/z = 278$), $[\mathrm{BIm{-}C_6H_4(NH)NC}]$ ($m/z = 160$), $[\mathrm{BIm{-}C_6H_4(NH)N.C.CH_2}]$ ($m/z = 146$), $[\mathrm{BIm{-}C_6H_4(NH)N.C.CH_2.NH}]$ ($m/z = 131$), $[\mathrm{BIm{-}C_6H_4(NH)N.C.CH_2.NH + H}]^+$ ($m/z = 132$), $[\mathrm{C_6H_4(NH)N + 3H}]^+$ ($m/z = 108$), $[\mathrm{C_6H_4(NH)N + 2H + Bz_3}]^+$ ($m/z = 261$), $[\mathrm{BIm + Bz_3}]$ ($m/z = 431$). UV–visible (CH_3OH) 390 nm ($\varepsilon = 1.5 \times 10^3$ $\mathrm{Lmol^{-1}\,cm^{-1}}$). ^1H NMR (CD_3OD, ppm) δ: 7.22 (*m*, 4H, ring proton), 7.53 (*m*, 4H, ring protons), 4.16 (*s*, 4H, $-CH_2-$). ^{13}C NMR (CD_3OD, ppm) δ: 140.5 $(C{=}N)_{im,}$ 115.2, 124.6,140 $(C{=}C)_{ar}$, 40.7 ($-CH_2-N$).

2.3. *Synthesis of [Fe(Im)Cl$_3$] (**1**) and [Fe(BIm)Cl$_3$] (**2**)*

A methanolic solution (10 mL) of anhydrous ferric chloride (0.64 g, 4.0 mmol) was dropped to a magnetically stirred solution of the ligand (4.0 mmol) taken in 60 mL methanol with stirring at room temperature. Reddish-yellow colour solution was formed after complete addition of the metal salt. The reaction mixture was stirred for ~2 days at room temperature, which gave yellow coloured precipitate. The precipitate was filtered off, washed with three portions of 2 mL methanol and dried in vacuo [m.p. 186 °C (**1**); 162 °C (**2**)]. Anal. Calc. for $C_{16}H_{15}N_5FeCl_3$: C, 27.94; H, 4.36; N, 20.37. Found for (**1**): C, 27.84; H, 3.31; N, 20.45. FAB-mass of (**1**) (*m*-nitrobenzylalcoho NBA, matrix): $[\mathrm{Fe(Im)Cl_3 + H}]^+$ $m/z = 343$, $[\mathrm{Fe(Im)Cl_2{-}H}]^+$ $m/z = 306$, $[\mathrm{Fe(Im)Cl}]^+$ $m/z = 272$, $[\mathrm{Fe(Im) + H}]^+$ $m/z = 238$. Anal. Calc. for $C_{16}H_{15}N_5FeCl_3$: C, 47.66; H, 3.72; N, 17.37. Found for (**2**): C, 47.23; H, 3.64; N, 17.24. FAB-mass of (**2**) (*m*-nitrobenzylalcoho NBA, matrix): $[\mathrm{Fe(BIm)Cl_3 + H}]^+$ $m/z = 439$, $[\mathrm{Fe(BIm)Cl_2}]^+$ $m/z = 403$, $[\mathrm{Fe(BIm)Cl}]^+$ $m/z = 368$, $[\mathrm{Fe(BIm) + H}]^+$ $m/z = 334$. [The spectra of the complexes contained bunch of peaks pertinent with the natural isotopes abundance ratio. The Fe as well as Cl nuclei are known to exhibit two naturally occurring isotopes with varying natural abundance. The m/z value of the isotope having highest intensity have been considered].

2.4. *Physico–chemical measurements*

IR spectra were recorded on a Perkin–Elmer spectrum GX automatic recording spectrophotometer as KBr disc. ^1H and ^{13}C NMR spectra of compounds dissolved in CD_3OD were recorded on a Brucker DRC-300 spectrometer using $SiMe_4$ (TMS) as internal standard. Electronic spectra of 10^{-3} M solutions in CH_3OH were obtained on a Cintra 5GBS automatic recoding spectrophotometer at room temperature. FAB-mass spectra were recorded on Jeol SX-102/DA-6000 mass spectrometer using argon (6 kV, 10 mA) as the FAB gas. The accelerating voltage was 10 kV and the spectra were recorded in *m*-nitrobenzyl alcohol (NBA) matrix. The matrix peaks appeared at $m/z = 136$, 137, 154, 289 and 307. Magnetic susceptibility on the solid complexes were made at RT by Gouy method using $Hg[CoNCS)_4]$ caliberant. The Mössbauer measurements were performed at IUC-DAE, Indore, India using a multi-channel analyzer in constant accelerating mode. The source was Co^{57} in Rh matrix (15 mci strength) and the instrument was caliberated with respect to natural Fe. The data were analyzed using least square program, NORMOS-SITE. Microanalysis for C, H and N were obtained from Microanalytical Laboratories, CDRI, Lucknow.

3. Results and discussion

The ligand, bis(4,5-dihydro-1*H*-imidazol-2-yl-methyl)amine (Im) was prepared employing a ring closure condensation reaction between iminodiacetic acid, $NH{-}(CH_2COOH)_2$ and 1,2-diaminoethane, $NH_2(CH_2)_2NH_2$ in presence of *ortho*-phosphoric acid under melt condition (~190 °C) in a closed reaction vessel (Section 2). The substituted analogue, bis(1*H*-benzimidazol-2yl-methyl)amine (BIm) was also obtained in an analogous manner using the aromatic analogue 1,2-diaminobenzene $NH_2C_6H_4NH_2$. The presence of *ortho*-phosphoric acid facilitates the condensation reaction as a catalyst affording a fairly good yield (yield > 60%) of the final products. The spectral studies presented here confirm the proposed ring closure mechanism as shown in Figure 1S (Supplemental Information) leading to the formation of (Im) or (BIm). The two imidazoline or benzimidazole rings of (Im) or (BIm) are bonded to a secondary amine function via methylene ($-CH_2-$) skeleton or linkage. The ligands provide three potential sites to coordinate Fe^{3+} ion as tridentate chelating ligand resulting in complexes of stoichiometry $FeLCl_3$ [L = Im (**1**) or BIm (**2**)].

3.1. *Analytical and FAB-mass spectral studies*

Analytical data of compounds are consistent with their proposed molecular formulae (Section 2). FAB-mass spectral data further supported the proposed stoichiometries of the compounds. FAB-mass spectrum of (BIm) exhibited a strong intensity (99% abundance) peak at $m/z = 278$ assignable to the molecular ion $[\mathrm{(BIm) + H}]^+$. However, for (Im) the spectrum peaks did not contain peaks assignable to any of the various probable molecular ions viz. $[\mathrm{(Im) + 2H}]^+$, $[\mathrm{(Im) + H}]^+$, $[\mathrm{(Im)}]^+$, $[\mathrm{(Im){-}H}]^+$ or $[\mathrm{(Im){-}2H}]^+$, expected at $m/z = 183$, 182, 181, 180 or 179, respectively. A low volatility coupled with a small thermal stability of the expected molecular ion (s) are usually responsible for an absence of the characteristic peak. It is possible that the molecular ion is quite reactive adding up with the matrix (NBA) fragments to generate the corresponding addition products [16]. The spectrum exhibited prominent peaks (~70% abundance) at $m/z = 333$, 472 and 490 assignable to $[(\mathrm{Im})–2\mathrm{H} + \mathrm{Bz}_3]^+$, $[(\mathrm{Im}) + 2\mathrm{H} + \mathrm{Bz}_4]^+$ and $[(\mathrm{Im}) + 2\mathrm{H} + \mathrm{Bz}_5]^+$, respectively, which are addition products of the molecular ion with the matrix fragments (Bz_3, Bz_4 and Bz_5). The observed high abundance (~70%) of the above peaks suggest that the addition products have good volatility. The spectra contained weak to strong intensity peaks due to species generated from the thermal fragmentations of the molecular ions.

The FAB-mass spectra of complexes (**1**) and (**2**) contained peaks at $m/z = 343$ and 439 consistent with the molecular ions $[\mathrm{Fe(Im)Cl_3}]^+$ and $[\mathrm{Fe(BIm)Cl_3}]^+$, respectively. These molecular ions further lose exocyclic ligands i.e. counter anions in a step-wise fragmentation process, which ultimately produce the corresponding species $[\mathrm{Fe(Im) + H}]^+$ ($m/z = 238$) and $[\mathrm{Fe(BIm) + H}]^+$ ($m/z = 334$). The FAB-mass spectral data of the complexes confirm that the present ligands provide strong chelation towards Fe^{3+}, which is considerably robust even under FAB-mass condition. The observed molar conductivities ($\Lambda\mathrm{m} = 30\,\mathrm{ohm^{-1}cm^2mole^{-1}}$) measured in DMSO indicate the non ionic nature [17] of the present complexes in solution.

3.2. IR spectral studies

IR spectra of ligands and the complexes $[\mathrm{Fe(Im)Cl_3}]$ (**1**) and $[\mathrm{Fe(BIm)Cl_3}]$ (**2**) contained absorption frequencies characteristic of the ν(C=N) and ν(C=C) stretching vibrations of the imidazoline or benzimidazole ring which are presented in Table 1S (Supplemental Information), along with their tentative assignments [18]. The spectra did not show the characteristic carboxylic group ν(C=O) and ν(O—H) stretching vibrations of the iminodiacetic acid reported to occur [19] in 1700–1800 $\mathrm{cm^{-1}}$ and 3400–3500 $\mathrm{cm^{-1}}$ regions, respectively. The absence of these bands along with the appearance of characteristic ring vibrations are in accordance with the proposed ring closure mechanism presented in Figure 1S (Supplemental Information). The additional strong intensity band observed at 3280 $\mathrm{cm^{-1}}$ is due to ν(N–H) stretching vibration of the secondary amine group [19,20]. The position of this band is significantly shifted ($\Delta\nu \cong 50\,\mathrm{cm^{-1}}$) to a lower frequency in the complexes relative to that in the free ligands. This negative shift is due to coordination of the metal ions to the secondary amine nitrogen. In addition the observed small positive shift ($\Delta\nu \cong 15–30\,\mathrm{cm^{-1}}$) in the characteristic ν(C=N) stretching vibration of the ring indicates additional coordinations from the pyridyl nitrogens of the imidazoline or benzimidazole ring [18]. A medium intensity band observed at 400 $\mathrm{cm^{-1}}$ in the complexes assignable [19,21] to the (M–N) bond stretching vibration. Furthermore, weak intensity bands in 230–250 $\mathrm{cm^{-1}}$ region is characteristic of (M–Cl) bond stretching vibration in the complexes. This is due to the presence of a considerable interaction between the counter $\mathrm{Cl^-}$ anions with Fe^{3+} ion of the complex cations $[\mathrm{Fe(L)}]^{3+}$. The counter $\mathrm{Cl^-}$ ion is known to behave as a weak exocyclic ligand towards the various transition metal ions [19] to result in a coordinatively saturated geometry (hexa-coordinate in the present case).

3.3. NMR spectral studies

The position with tentative assignments [22] of the ^{1}H and ^{13}C NMR resonance signals observed in the spectra of the ligands are summarized in the Section 2. The imidazoline ring $–\mathrm{CH_2}–$ protons resonances in (Im) appeared as two separate equal intensity symmetrical triplets. However, for (BIm) the observed two well resolved equal intensity symmetrical multiplets are characteristic of aromatic protons in AA′, BB′ environments of the substituted benzene rings [23]. The symmetrical nature of the observed resonance peaks suggests presence of a two fold C_2 symmetry axis and σ_v symmetry mirror planes characteristic of C_{2v} point group of the molecular symmetry. The spectra contained an additional singlet in 4.1–4.5 δ region assignable to the skeleton $–\mathrm{CH_2}–$ protons bond to secondary amine function. Signal due to NH protons was not indicated probably, due to a fast proton exchange coupled with the quadrupole relaxation effect [24] of N ($I = 1$). However, for the complexes the observed broad undefined feature for the resonance peaks is due to paramagnetic effect of Fe^{3+} [25].

3.4. Electronic (ligand field) spectral studies

The electronic spectra of (Im) and (BIm) recorded in $\mathrm{CH_3OH}$ exhibited a strong intensity band ($\varepsilon \cong 1.5 \times 10^3\,\mathrm{Lmol^{-1}\,cm^{-1}}$) at 390 nm (25.640 $\mathrm{cm^{-1}}$) and 398 nm (25.130 $\mathrm{cm^{-1}}$), respectively, which is attributed [26,27] to an electronic transition form the filled π orbital (HOMO) to the empty π^* orbital (LUMO) i.e. $\pi \to \pi^*$ transition of the iminic (C=N) function present in the ligand moiety. The electronic spectra of complexes contained three relatively weak intensity bands ($\varepsilon \cong 10–50\,\mathrm{Lmol^{-1}\,cm^{-1}}$) characteristic of ligand field (d–d) transitions [28] in addition to a broad strong intensity band due to the ligand $\pi \to \pi^*$ transition in conjugation with the metal ← ligand (M ← L) charge transfer transition band. In complexes the position of $\pi \to \pi^*$ transition band is red-shifted (shift to higher wavelength or lower energy) compared to that observed in the free ligand. This shift to lower energy indicates either a stabilization of π^* (LUMO) or destabilization of π (HOMO) after complexation with the metal ion. The metal (dπ)–ligand (π^*) overlap, which enhances the extent of back donation usually lowers the energy or stabilizes the HOMO. The observed ligand field (d–d) bands are characteristic of an octahedral coordination around high-spin Fe^{3+} ion whose position along with assignments have been summarized in Table 2S (Supplemental Information). We could not succeed in obtaining single crystal suitable for X-ray crystallographic studies even after repeated recrystallization. However, molecular model computations discussed below have enabled us to propose theoretical perspective regarding the most probable shapes of the ligands and their complexes.

3.5. Molecular modeling studies

The molecular model computations based on CSChem-3D-MOPAC were employed [29,30] to solve probable molecular structures of the ligands [(Im) & (BIm)] as well as of the complexes (**1**) and (**2**). The mechanical adjustments via augmented mechanical fields were used to draw the optimized minimum energy plots, as shown in Figs. 1–4. The plots (Figs. 1 and 2) indicate that the potential donor aza atoms in the ligands (Im) and (BIm) do not lie in same plane, as the energy requirement for such an arrangement would involve high energy. Furthermore, in complexes (**1**) and (**2**) the ligands behave as a tridentate [N,N,N] chelating agent, and the hexa-coordinate geometry around Fe^{3+} is achieved through additional coordination from the counter chloride ion. The appearance of weak intensity bands in 230–250 $\mathrm{cm^{-1}}$ region characteristic of ν(M–Cl) stretching vibration [19] in the IR spectra of complexes supported coordination from the $\mathrm{Cl^-}$ counter anion. The ligands bind Fe^{3+} in mer. arrangement as the most probable mode of coordination (Figs. 3 and 4) because the aza donor sites [N,N,N] are away from the coplanarity. The alternative fac. arrangment requires a coplanarity of all the bonded aza sites has a high-energy involvement and therefore it is less probable. The computed important bond lengths and bond angles in the molecules are presented in Table 3S (Supplemental Information).

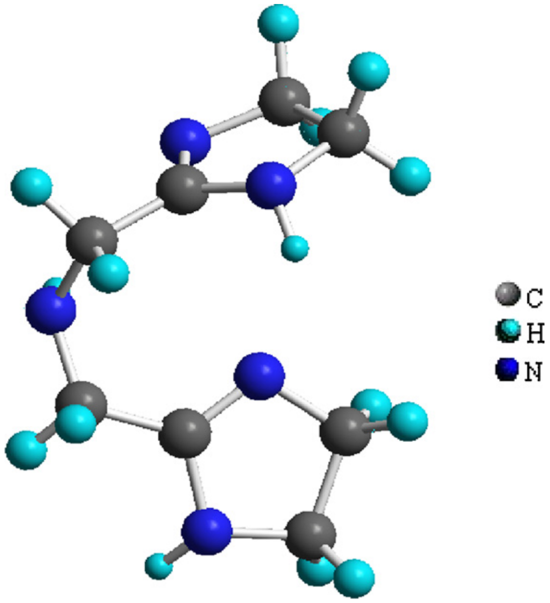

Fig. 1. The perspective view of the ligand (Im).

3.6. Mössbauer and magnetic moment studies

The ^{57}Fe-Mössbauer spectral informations coupled with the magnetic moment data provide ample idea about the molecularity as well as the coordination geometry. The observed representative Mössbauer spectra along with the important computed parameters like isomer shifts (δ), quadruple splittings (ΔE_Q), line widths and peak height ratio (HW_h/HW_l) of (**1**) and (**2**) are shown in Figs. 5 and 6, respectively. The least square fit methodology employing Lorentzian line shape was used for the spectral plots, which clearly indicate that the spectra contained only one type quadrupole split doublet. This is consistent with the presence of only one electronic and stereo–chemical environment around iron nucleus in the lattice of the complex moiety. The magnitude of isomer shift (δ) and the quadrupole splitting (ΔE_Q) parameters of the present complexes are in the range [31] of the various high-spin state Fe^{3+} nuclei ($t_{2g}{}^3$,$e_g{}^2$) in a hexa-coordinate environment of the ligands. This indicates that Fe^{3+} ion in the present complexes acquire [31] a high-spin state ($S = 5/2$) rather than a low-spin ($S = 1/2$) ground state electronic configuration ($t_{2g}{}^5$). The magnetic moment studies of (**1**) and (**2**) further confirmed the high-spin state of the metal ion. The observed magnetic susceptibility (μeff. ≅ 6 BM) as summarized in Table 3S (Supplemental Information) are comparable to the spin-only moment (μso ≅ 5.9) for five unpaired spins in a high-spin state of Fe^{3+} [32]. The magnetic moment for low-spin state configuration of d^5 ($t_{2g}{}^5$) system, which

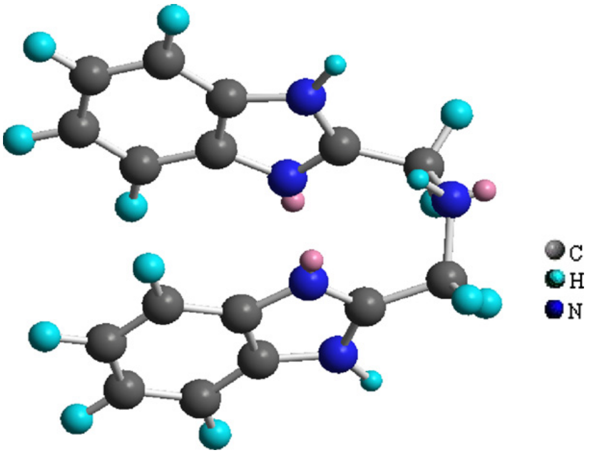

Fig. 2. The perspective view of the ligand (BIm).

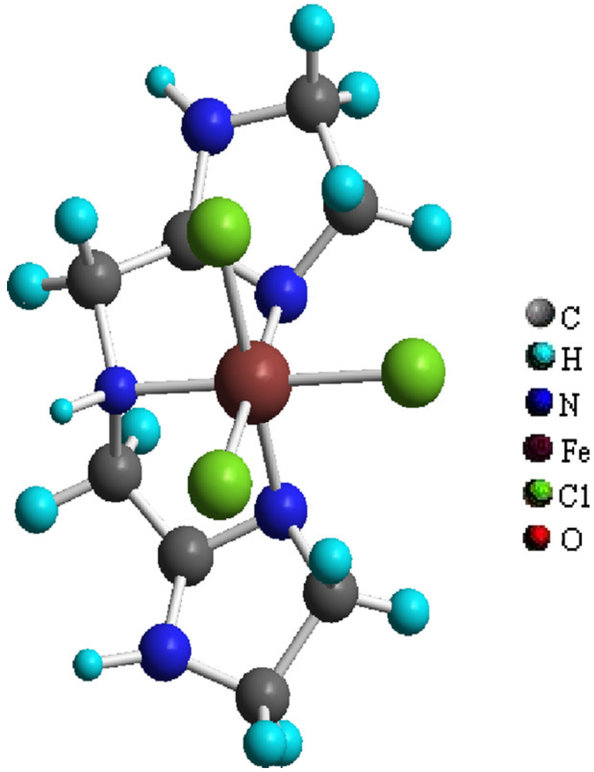

Fig. 3. The perspective view of the complex [$Fe(Im)Cl_3$] (**1**).

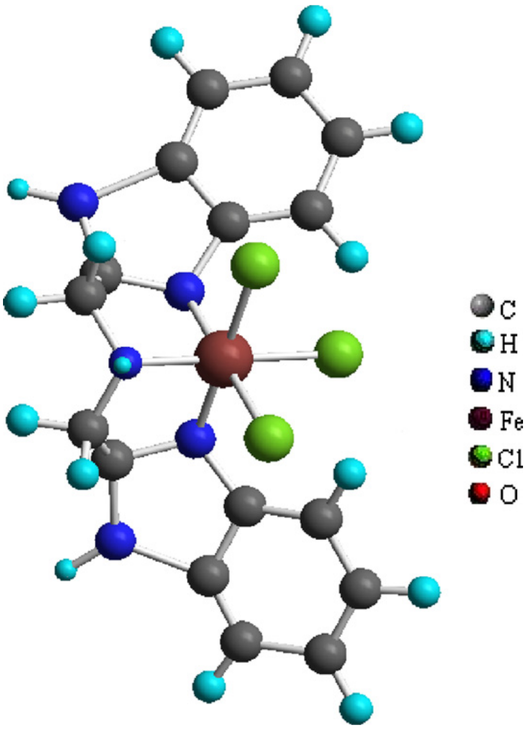

Fig. 4. The perspective view of the complex [$Fe(BIm)Cl_3$] (**2**).

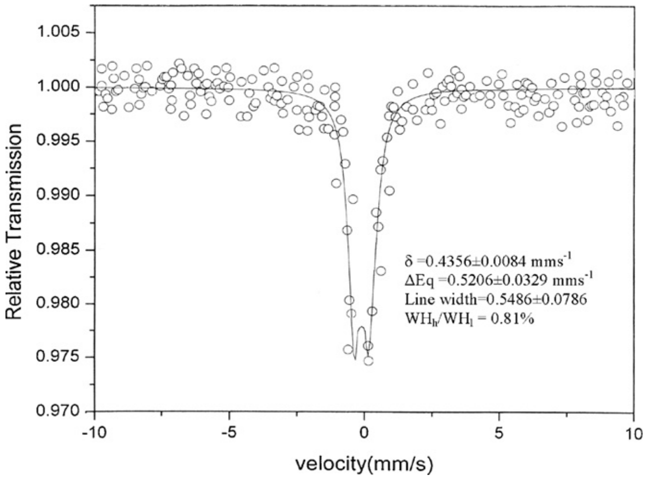

Fig. 5. Representative Mössbauer spectrum for the complexes (**1**) with the corresponding Mössbauer parameters recorded at 298 K.

effectively contains only one unpaired spin requires μeff. ≅ 2.0 BM. This is far from the observed μeff. value, henceforth, ruled out its possibility. The quadrupole doublets are symmetrical in nature which did not support the presence of any fluctuating electric or magnetic field near the Mossbauer Fe^{3+} nucleus and moreover, there is a possibility of the spin-lattice relaxation [31,33]. The average peak position (δ) is in the positive side indicating that the *s* electron density on the metal ion is smaller [31] in the complexes relative to that of the source. The observed peak height ratios (WH_h/WH_l) are comparable to that reported [34] for the monomeric high-spin Fe(III) complexes. The magnitude of δ determines the coordination geometry which varies in the order: eight-coordinate > six-coordinate > four-coordinate [34] such that for six-coordinate geometry it is close to 0.6 mm s^{-1} [35]. An increase in the extent of distortion from perfect octahedral (O_h) symmetry tends to lower the magnitude of δ even in a six-coordinate Fe(III) complex such that it can attain a magnitude close to that of the four-coordinate geometry (i.e. $\delta < 0.4$ mm s^{-1}). In the present complexes, too the observed magnitude of δ indicates a considerable distortion in the over all geometry around Fe^{3+} ion. This produces a considerable ligand field asymmetry, causing the quadrupole splitting even in the high-spin (d^5,$t_{2g}{}^3$,$e_g{}^2$) state electronic configuration of Fe^{3+}. The quadrupole split peaks lie in the positive direction of the zero velocity which reflects that the Mössbauer nuclear excitation involve transition from high-energy ($I = \pm3/2$) to low-energy ($I = \pm1/2$) i.e. the effective nuclear transition is Fe ($\pm3/2 \rightarrow \pm1/2$). The application of external magnetic field did not affect any further magnetic splitting suggesting that the nuclear magnetic field near the Mössbauer nucleus is either absent or it is too low to show any significant interaction such that the spin states remain doubly degenerate (i.e. presence of Kramer's degeneracy).

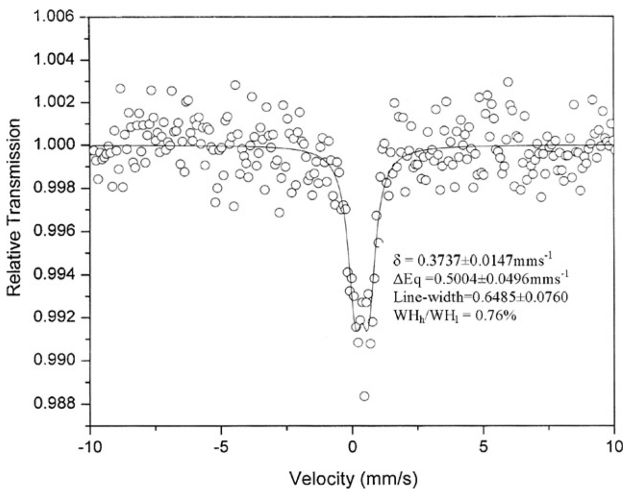

Fig. 6. Representative Mössbauer spectrum for the complexes (**2**) with the corresponding Mössbauer parameters recorded at 298 K.

Acknowledgments

The authors are thankful to Chairman, Department of Chemistry, Aligarh Muslim University, Aligarh, India, for providing necessary research facilities and to Prof. A. Gupta for recording the ^{57}Fe spectra at the IUC facilities, Indore, India. Financial support from University Grant Commission, New Delhi, India, in the form of a Research Grant was gratefully acknowledged.

Appendix A. Supplementary data

Supplementary data associated with this article can be found, in the online version, at doi:10.1016/j.saa.2008.07.016.

References

[1] J.J.R. Fausto da Silva, R.J.P. Williams, The Biological Chemistry of the Elements, The Inorganic Chemistry of the Life, Clarendon Press, Oxford, 1991.
[2] S. Chen, J.F. Richardson, R.M. Buchanan, Inorg. Chem. 33 (1994) 2376.
[3] L.P. Wu, Y. Yamagiwa, I. Ino, K. Sugimoto, T. Kuroda-Sowa, T. Kamikawa, M. Munakata, Polyhedron 18 (1999) 2047.
[4] N. Wei, N.N. Murthy, Z. Tyeklár, K.D. Karlin, Inorg. Chem. 33 (1994) 1177.
[5] K.J. Oberhausen, R.J. O'Brian, J.F. Richardson, R.M. Buchanan, Inorg. Chim. Acta 173 (1990) 145.
[6] E. Quiroz-Castro, S. Bernes, N. Barba-Behrens, R. Tapia-Benavides, R. Contreras, H. Nöth, Polyhedron 19 (2000) 1479.
[7] C.-Y. Su, B.-S. Kang, T.-B. Wen, Y.-X. Tong, X.-P. Yang, C. Zang, H.-Q. Liu, J. Sun, Polyhedron 18 (1999) 1577.
[8] G.J.A.A. Koolhaas, W.L. Driessen, J. Reedijk, J.L. van der Plas, R.A.G. de Graaff, D. Gatteschi, H. Koojiman, A.L. Spek, Inorg. Chem. 35 (1996) 1509.
[9] R.H. Holm, P. Kennepohl, E.I. Solomon, Chem. Rev. 96 (1996) 2239.
[10] I. Török, P. Surdy, A. Rockenbauer, L. Korecz, G.J.A.A. Koolhaas, T. Gajda, J. Inorg. Biochem. 71 (1998) 7.
[11] K.D. Karlin, P.L. Dahlstrom, M.L. Stanford, J. Zubieta, Chem. Soc. Chem. Commun. (1979) 465;
K.D. Karlin, P.L. Dahlstrom, J.R. Hyde, J. Zubieta, Chem. Soc. Chem. Commun. (1980) 906.
[12] R.W. Hay, T. Clifford, P. Lightfoot, Polyhedron 17 (1998) 4347.
[13] A.M. Dittler-Klingemann, C. Orvig, F.E. Hahn, F. Thaler, C.D. Hubbard, R. van Eldik, S. Schindler, I. Fábián, Inorg. Chem. 35 (1996) 7798.
[14] F. Thaler, C.D. Hubbard, F.W. Heinemann, R. van Eldik, S. Schindler, I. Fábián, A.M. Dittler-Klingemann, F.E. Hahn, C. Orvig, Inorg. Chem. 37 (1998) 4022.
[15] W.L.F. Armarego, D.D. Perkin, Purification of Laboratory Chemical, 4th ed., Butterworth-Heinemann, 1997.
[16] Z.A. Siddiqi, M.M. Khan, Synth. React. Inorg. Met-Org. Chem. 34 (2004) 897.
[17] W.J. Geary, Coord. Rev. 7 (1971) 81.
[18] J. Reedijk, J.K. DeRidder, Inorg. Nucl. Chem. Lett. 12 (1976) 585.
[19] K. Nakamoto, Infrared and Raman Spectra of Inorganic and Coordination Compounds, Wiley-Interscience, New York, 1986.
[20] T. Kurisaki, T. Yamaguchi, M. Fujiwara, R. Kiraly, H. Wakita, J. Chem. Soc., Dalton Trans. (1996) 3727.
[21] Z.A. Siddiqi, R. Arif, S. Kumar, M. Khali, Spectrochim. Acta A 70 (2008) 1193–1197.
[22] Z.A. Siddiqi, R. Arif, S. Kumar, M. Khalid, J. Coord. Chem. 61 (2008) 2032.
[23] L.K. Thompson, B.S. Ramaswamy, E.A. Seymour, Can. J. Chem. 55 (1977) 878.
[24] R.S. Drago, Physical Methods for Chemistry, Sannders College Publishing, New York, 1992, 500 pp.
[25] S.J. Feruson, Metal Ions as NMR Probes in Biochemistry, in: C.A.M. Auliff (Ed.), The Techniques and Topics in Bioinorganic Chemistry, Mac Miltan Press Ltd., London, New York, 1975, p. 307.
[26] K. Motrado, H. Sakiyama, N. Matsumoto, H. Okawa, D. Fenton, J. Chem. Soc., Dalton Trans. (1995) 3419.
[27] C.N.R. Rao, Ultra-violet and Visible Spectroscopy, Butterworth & Co. Ltd., London, 1994.
[28] A.B.P. Lever, Inorganic Electronic Spectroscopy, 2nd ed., Elsevier, Amsterdam, 1984.

[29] J.J.P. Steward, J. Comp. Chem. 10 (1989) 221.
[30] D. Hinks, J. Lye, H.S. Freeman, Computer Aided Dyestuff Design Book of Paper—AATCC, International Conference and Exhibition, Atlanta, Georgia, 1995, 74 pp.
[31] N.N. Greenwood, T.C. Gibbs, Mössbauer Spectroscopy, Chapman and Hall Ltd., London, 1976.
[32] J. Lewis, R.G. Wilkins, Modern Coordination Chemistry, Interscience Publisher, New York, 1960.
[33] M. Bhime, J.A. Jhon, Phys. Rev. 165 (1968) 446.
[34] G.M. Bancroft, R.G. Burns, A.G. Maddock, Geochim. Cosmochim. Acta 31 (1967) 2219.
[35] G.M. Bancroft, A.G. Maddock, W.K. Ong, R.H. Prince, J. Chem. Soc. (1966) 723.